

## Facile Synthesis, Characterization and Photocatalytic activity of MOF-5

Manisha A. Bora<sup>1\*</sup>, Suhani Patel<sup>1</sup>, Parag Adhyapak<sup>2</sup>

<sup>1</sup> Department of Chemistry, BJS'S ASC College, Nagar Road, Wagholi, Pune-412207

<sup>2</sup> Centre for Materials for Electronics Technology (C-MET) Panchawati, off Pashan Road, Pune-411008

\*Email- bmanishabora@gmail.com,

Received: 5.1.2025, Revised: 6.1.2025, 19.1.2025, 22.1.2025 Accepted: 25.1.2025

### Abstract:

Metal–Organic-Frameworks (MOFs) are highly tunable to design and functionalize, hence they are recognized as materials of interest in applied sciences. MOF-5 having formula  $(Zn_4O_{13}-(C_8H_4)_3)$ , is a well-known MOF due to its distinctive porosity and thermal stability. MOF-5 has a 3D structure comprising of terephthalic acid and  $Zn_4O$  clusters. In the present study, the MOF-5 was synthesized using facile, ecofriendly one pot hydrothermal process at low temperature. The MOF-5 was characterized to assess intrinsic properties such as crystallinity, morphology, functional groups at surface sites, using techniques like UVDRS, FTIR, XRD and FESEM. The synthesized material was also verified for its photocatalytic activity towards dye degradation of methyl orange (MO). The synthesized material of MOF-5 displays excellent MO dye deprivation efficiency in a natural sunlight by facilitated photodegradation route.

**Keywords:** porous material, MOF-5, dye degradation, methyl orange (MO)

### 1. Introduction:

In recent times, the field of Metal Organic Frameworks (MOFs) has become one of the foremost survey stresses in assorted fields of investigation. MOF is a coordination complex with organic ligands comprising prospective cavities. MOF-5 comprises of tetrahedral  $[Zn_4O]^{6+}$  masses associated by benzene dicarboxylic acid linkers (BDC) to form a 3D cubic complex. These materials which are prepared by associating inorganic and organic units show pronounced flexibility with which the components geometry, size, and functionality can be varied<sup>1-3</sup>. Metal-organic frameworks symbolize porous materials that are building up from

metal ions or metallic complexes and organic ligands. Organic molecules containing one or more N-donor or O-donor atoms are normally used as organic ligands to bridge between the metal ions in MOFs. Carboxylates, pyridyl and cyano compounds, oxalic acid, and benzene, phosphonates, sulfonates, and crown ethers are the most common ligands used. The anions counterbalance the positive charge of cationic MOFs and influence the supra molecular structure either being coordinated to the metal ions or by occupying the pores of the structure<sup>4-6</sup>. The 3D assembly of MOFs is designed due to robust coordination bonds between the metal ions and the organic ligands and displays voids and inner surfaces, which are occupied by counter ions, guest molecules, and/or solvate molecules. Other types of interactions, such as hydrogen bonds, metal-metal bonds, and  $\pi$ - $\pi$  interactions can occur and contribute to the stability of the MOFs. The post-synthetic alteration of the MOFs later their production has been widely used to introduce functional assemblies and give the anticipated physico-chemical properties<sup>7-9</sup>. The possibility of functionalization of the size and shape of the pores compromises high potential for solicitations in the energy and environment, with gas sorption, storage, and separation, as well as metal ions and toxic molecules for analytical and sensing dedications, insertion of drugs, and biologically important molecules as smart transporters for anti-cancer and anti-microbial remedies. Since the novelty of these spongy porous materials, their hopeful solicitations in several fields such as, gas storage, energy storage, catalysis, dye degradation, drug synthesis, etc., remain to spread and have drawn commitment of investigators for innovative analysis and uses. High porosity gives these materials a high-class distinguishing possession<sup>10-14</sup>. In the present work by considering the remarkable photocatalytic possessions of Zn-based MOFs, the present work focuses on facile synthesis of MOF-5 and its application as a photocatalyst for MO dye degradation was evaluated. The photodegradation action of the prepared MOF-5 sample was inspected against methylene Orange (MO) dye in presence of natural sunlight. It is exciting to find that the alteration in morphology and elemental content has extraordinary consequence on photocatalytic activity of the MOF-5 material for dye degradation phenomenon. The current work highlights the solicitations of MOF-5 for MO degradation in sunlight.<sup>15-21</sup>

## **2. Experimental Section**

### **2.1 Materials and methods**

The entire chemicals castoffs for the production of MOF-5 were of AR grade. Benzene dicarboxylic acid (BDC), zinc acetate dihydrate, N, N-dimethyl formide (DMF), ethanol, methyl orange, and DI water were used for the synthesis and degradation studies obtained

from SD Fine India Ltd. All the chemicals were used as received without any additional purification.

## **2.2 Synthesis of MOF-5**

MOF-5 was synthesized according to a modified hydrothermal method. Zinc acetate (3.83 mmol, 0.85g) and Benzene dicarboxylic acid (BDC) (5.30 mmol, 0.95g) were dissolved in 7 ml N, N-Dimethyl formide (DMF) and 3 ml ethanol (ratio of 7:3) in a conical flask with constant stirring up to 2.5 hour at room temperature. After stirring, the mixture was centrifuged for 5 min at 2000 rpm. Then it was heated hydrothermally at 80°C for 2 hrs. The reaction mixture was then cooled and filtered. The solid product obtained was then washed with DMF and dried in oven. Analytical technique namely, UV-Vis, FTIR, XRD and FESEM were used confirm the various properties of synthesized material of MOF-5.

## **2.3 Study of photocatalytic performance of MOF-5**

In the present work, the effect of initial photo catalyst (MOF-5) concentration under direct sunlight irradiation was inspected by changing the initial concentration from 10 to 50 mg per 100 ml of 10 mg methyl orange (MO) dye solutions. After adding MOF-5 to methyl orange solution, it was exposed to ultrasonication for 1 minute to get uniform mixture. The solution mixture was agitated in the dark for 20-30 min to attain adsorption-desorption equilibrium. Then absorbance was found out in colorimeter without keeping the test-tube in the sunlight. After taking absorbance test-tube was kept in the sunlight for photodegradation of MO and absorbance was taken every day for consecutive 10 days. All the observations were noted for 0.05M, 0.1M and 0.5M concentrations of the MO. The above method was repeated to obtain the data for dye degradation under dark circumstances.

## **2.4 Characterization**

The pure MOF-5 was characterized to investigate its intrinsic possessions using different instrumental methods. UV-visible absorption measurements were taken by a UV-VIS-NIR spectrophotometer (SHIMADZU Pharmespec UV-1700). The UV-Vis spectroscopy was carried out in the range of 200–700 nm. The functional groups of MOF-5 was recognized using Fourier transform infrared (FTIR, Perkin Elmer/Spectrum II) spectrometer using ATR disc mode in the range of 500–4000cm<sup>-1</sup> wavenumber. The powder X-ray diffraction (PXRD) data was collected using Rigaku Miniflex diffractometer in the angular range of 2θ = 10–70°

with CuK $\alpha$  radiation ( $\lambda = 1.5418 \text{ \AA}$ ; nickel filter) and the scan speed of  $1^\circ \text{ min}^{-1}$ . The morphological studies were accompanied using field scanning electron microscopy (FESEM) (Hitachi Model 5890).

### 3. Results and Discussion:

The synthesized MOF-5 material was characterized by several characterization implements to recognize its structural and morphological feature which ultimately impacting its catalytic activity. The absorption spectrum of MOF-5 was recorded using distilled water as reference. The structural analysis of MOF-5 samples was carried out via UV, FTIR, XRD and SEM techniques.

The UV-Vis spectra (Fig.1) of MOF-5 displays maximum absorption at 300nm agrees to the  $\pi-\pi^*$  transition demonstrated by the  $\pi$  electrons of 1, 4-benzene dicarboxylic acid i.e. BDC ligand in MOF-5 and corresponds to  $1A_{1g}$  to  $1B_{2u}$  excitation.

FTIR investigation (Fig.2) shows the FTIR spectrum of the synthesized MOF-5. The peak at  $3450\text{cm}^{-1}$  belongs to O-H group. The peak located in  $1350\text{cm}^{-1}$  relates to the symmetrical vibration of the carboxyl group and the other peak observed in  $1600\text{cm}^{-1}$  are allocated to the asymmetric vibrations of the -COOH group which is one of the chief groups of terephthalic acid ligand. The peaks in  $640$ ,  $850$  and  $1010\text{cm}^{-1}$  can be assigned to the bending vibration of the C-H bond. The peak centered at  $530\text{cm}^{-1}$  is assigned to the Zn-O vibration in the  $\text{Zn}_4\text{O}$  group. Fourier transform infrared (FTIR) spectrum of MOF-5 displays strong bands at  $1659$  and  $1600\text{cm}^{-1}$ , which match to the C=O and C-O group stretching vibration of the aromatic ring of terephthalic acid.

The PXRD pattern of MOF-5 shows (Fig.3) a peak at  $2\theta = 9.8^\circ$  which corresponds to the MOF-5 crystal plane. A peak at  $6.1$ ,  $9.8$ ,  $13.1$ ,  $15.6^\circ$  belongs to (200), (220), (400), (420) planes as mentioned in the literature<sup>17-20</sup>. As shown in Fig.3, the key diffraction peaks at  $6.1^\circ$  and  $9.8^\circ$  approve the successful creation of MOF-5 crystalline phase. The intensity ratio of the powder XRD peak at  $9.8^\circ$  to the peak at  $6.1^\circ$  (denoted to as the R1 value) can be castoff to guess the adsorption possessions of a MOF-5 like materials. From the PXRD pattern of the material it is clear that the R1 value of the material is low which is responsible for the dye photodegradation properties of the synthesized MOF-5. Moreover the small R1 value, the intensity of the peak at  $13.1^\circ$  is high, which relates to the reflections of (400) planes of the cubic structure of MOF-5.<sup>21</sup> By using Debye Scherrer equation ( $D = k \lambda / \beta \cos\theta$ ) the particle

size was of MOF-5 material was calculated. The average crystallite size of MOF-5 was found to be 60-140nm.<sup>22</sup>

FESEM images of MOF-5 have been represented in Fig.4. It is observed that the MOF-5 is generated of a large number of elliptical petals like structures as shown. The petals like constructions witnessed in the synthesized MOF-5 are found to be organized in regular assemblies which is distinctive in these 2D structures and in line with the previous reports<sup>13-16</sup>.

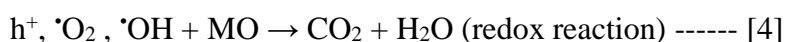
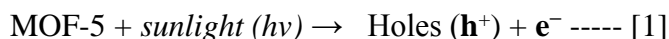
### **3.1 Photocatalytic activity of Methyl Orange (MO)**

The dye manufacturing alone is majorly accountable for widespread ecological destruction. As a consequence, it is vital to improve novel approaches to eradicate these pollutants from water bodies entirely. Amongst numerous methods established, photo catalytic degradation has received distinct devotion due to its small cost, modest process, abolition of secondary pollutants, and operative elimination of contaminants. Keeping these things in mind the prepared sample of MOF-5 was tested for the dye photo degradation study. The methyl orange dye degradation was carried out as explained in procedure. The results obtained after 1, 4, 6 and 10 days are displayed in photographs. MO is a common organic dye, and it is very interesting to decompose it from wastewater. The photocatalytic activity of the MOF-5 is examined by revealing the MO solution comprising photocatalyst to natural sunlight radiation. There is a decrease in the peak intensities of absorption spectra (Fig.5) demonstrating the decomposition of the organic pollutant. The graph of concentration versus absorbance and time versus absorbance were plotted as shown in Fig.5 and 6 for both i.e. for reference and MOF-5. The synthesized material (MOF-5), due to its high photocatalytic activity can be efficiently cast-off for degradation of MO dye.<sup>17</sup> It was observed that for complete MO dye degradation in presence of MOF-5 and natural sunlight, it required three to five days for various concentrations (0.05-01M) of the MO samples. Furthermore, when MO solutions of various concentrations were exposed to sunlight in absence of MOF-5, it was observed that about seven to ten days were required for complete dye degradation. It was also observed that when the amount of photocatalyst was increased from 10 to 50 mg, the photocatalytic activity was found to be increasing, which could be caused by an increased number of active sites on the catalyst surface. Further increase in the catalyst amount above 50 mg diminished the activity, which could be due to the phenomenon of light scattering. Specifically, this can be attributed to the increased collection of particles acting as obstacles

for the light irradiation<sup>17-20</sup>. The optimum activity of synthesized MOF-5 was observed when 50mg of the material was taken in various concentrations of MO in presence of sunlight. In absence of sunlight, no dye degradation activity of MOF sample was observed.

### 3.2 Mechanism of photo catalysis under sunlight using MOF

The photo dye degradation includes a practice in which the catalyst absorbs energy in the form of sunlight to produce extremely reactive free radicals in a sequences of red-ox reactions. If a material is exposed to sunlight, it absorb radiations and causes electronic excitation, generating an electron-pair hole in its conduction band and valence band. These sunlight created holes can oxidize H<sub>2</sub>O molecules adsorbed on the surface of catalyst to produce (OH<sup>•</sup>) radicals. Then, these ROS i.e. Reactive Oxygen Species may oxidize the dye molecules into smaller species which are harmless. MOF-based constituents display analogous properties as semiconductor photo catalysts. The valence band corresponds to the HOMO of the MOF, whereas the conduction band corresponds to the LUMO. Beneath light radiations, electrons are promoted from the HOMO of the ligand (BDC) and transitioned into the LUMO of the metal (Zn) as shown in Fig 7. The complete mechanism may be assumed from the following sequence of Red-ox reactions<sup>22</sup>.



### 4. Conclusion

In summary, we have synthesized the MOF-5 material using DMF as the solvent and fully characterized. The MOF-5 was designed by the facile, ecofriendly hydrothermal method and exploited as a photocatalyst. The successful preparation of MOF-5 nano-petals was confirmed through the numerous advanced analytical methods such as UV, FTIR, PXRD, and FE-SEM analysis. The photocatalytic properties of MOF-5 were confirmed by dye degradation study of methyl orange in natural sunlight. From the results obtained we can confirm that synthesized MOF-5 material has good porosity and hence can be successfully exploited for the MO degradation in presence of sunlight in small amount. It took about three to five days for complete MO dye degradation having concentrations 0.05M, 0.1M and 0.5M when exposed to 50mg of MOF-5 sample in presence of sunlight.

Figures:

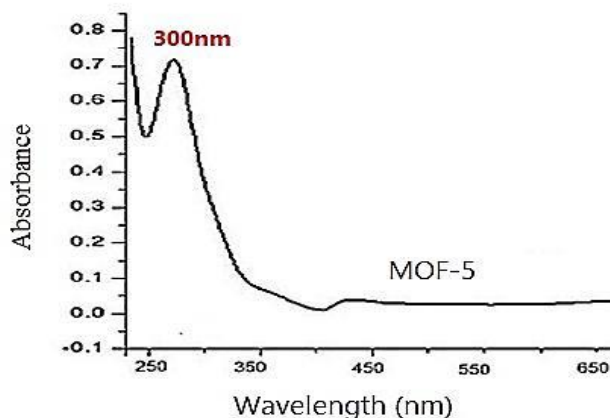


Fig.1 UV-Vis spectra of MOF-5

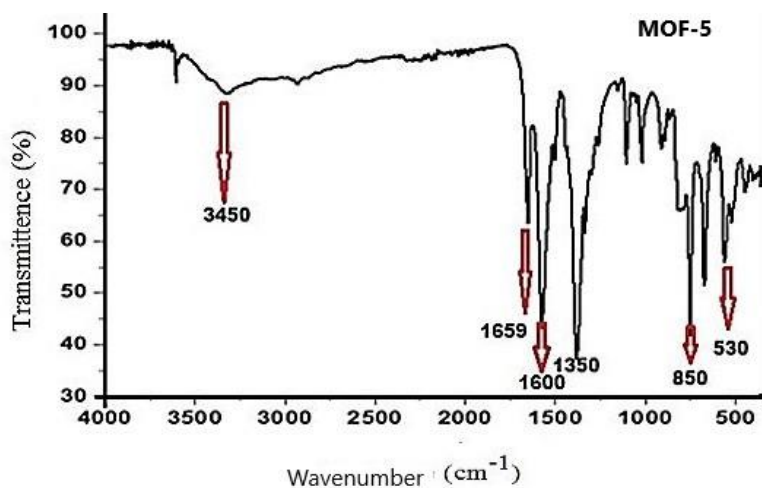


Fig.2 FTIR spectra of MOF-5

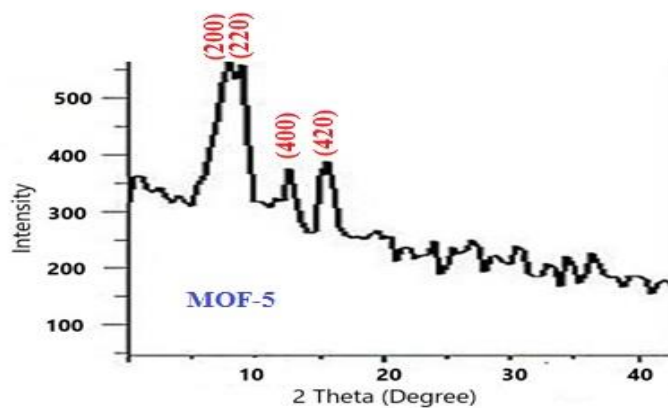


Fig.3 XRD spectra of MOF-5

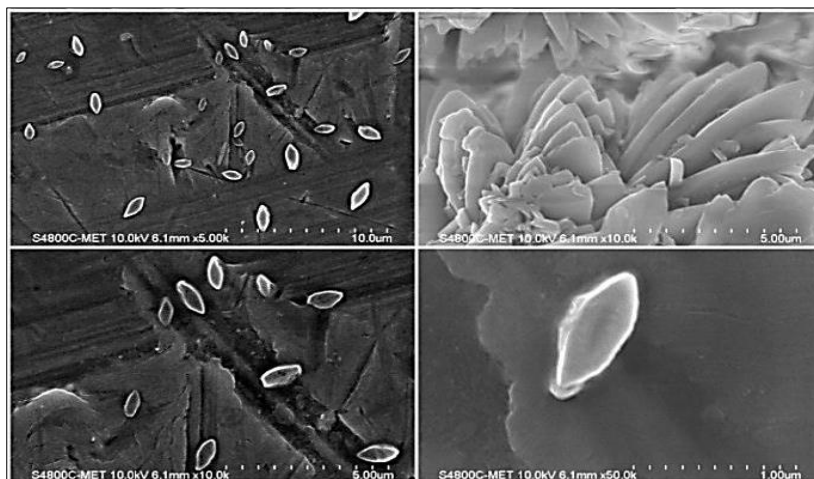


Fig.4 FESEM images of MOF-5

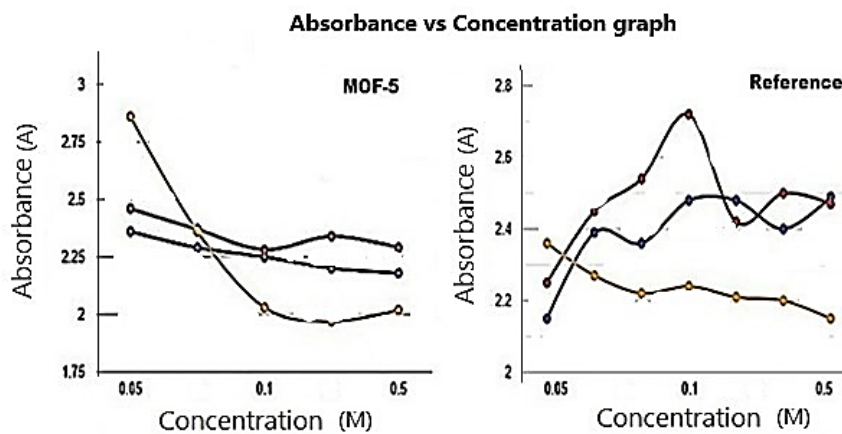


Fig.5 Absorption versus Concentration graph

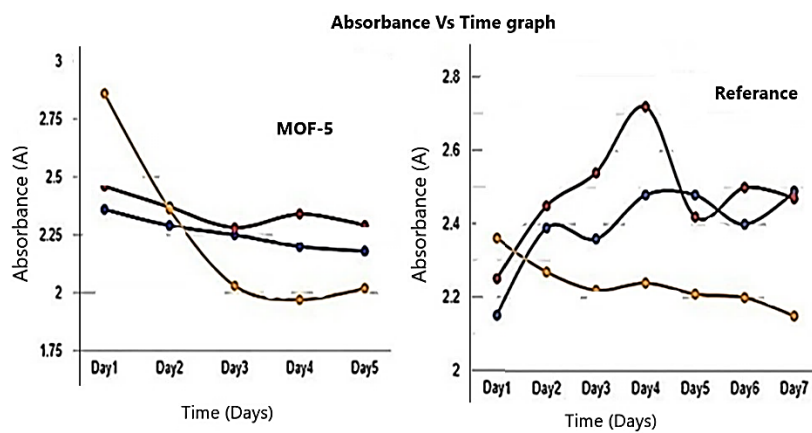


Fig.6 Absorbance versus Time graph





MO dye degradation study

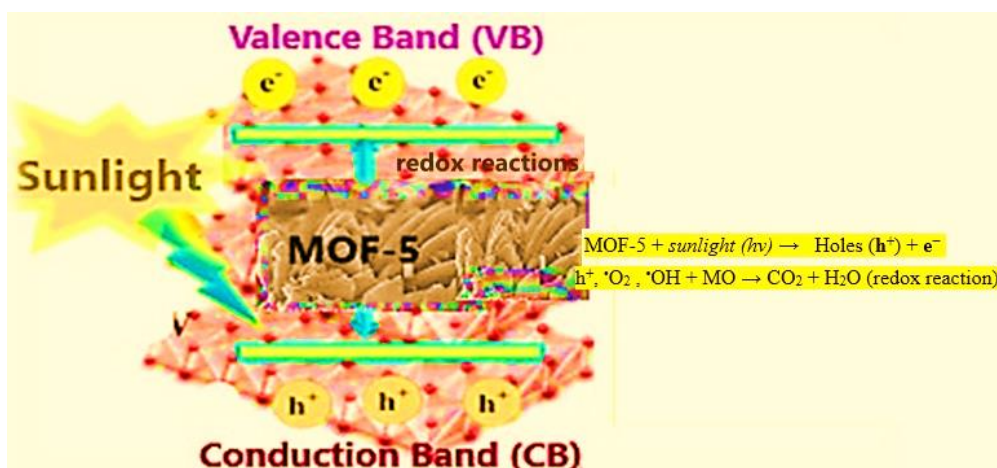


Fig.7 Mechanism of photocatalysis of MOF-5 under sunlight

**References:**

1. A. Chakrabortya and H. Achary, New J. Chem., 47, 1498, 2023.
2. B. Tabasum, P. Dhagale, K. Nitnaware, H. Nikule, T. Nikam, J. Environ. Chem. Eng.,7(3), 103114, 2019.
3. M. Suleman, M. Zafar, A. Ahmed, M. Rashid, S. Hussain, A. Razzaq, N. Mohidem, T. Fazal, B. Haider, Y. Park, Sustainability, 13(12), 6926, 2021.
4. S. Singh, S. Perween, A. Ranjan, J. Environ. Chem. Eng.,9 (3), 105149, 2021.
5. H. Zhao, H. Song, L. Chou, Inorg. Chem. Commun., 15, 261, 2012.
6. T. Zhang, W. Li, Q. Guo, Y. Wang, C. Li, Coatings, 12, 559, 2022.
7. X. Chen, Y. Zhang, X. Kong, K. Yao, L. Liu, J. Zhang, Z. Guo, W. Xu, Z. Fang, ACS Omega, 6, 2882, 2021.

8. A. Anum, M.A. Nazir, S.M. Ibrahim, S.S.A. Shah, A.A. Tahir, M. Malik, M. A. Wattoo, A. Rehman, *Catalysts* 13, 9849, 2023.
9. C. C. Wang, X. H. Yi, P. Wang, *Appl. Catal. B Environ.* 247, 24, 2019.
10. P. Koochi, A. Rahbar-kelishami, H. Shayesteh, *Environ. Technol. Innov.*, 23, 101559, 2021.
11. R. Ahmad, Z. Ahmad, A. Ullah, N. Riaz, M. Aslam, *Environ. Chem. Eng.*, 4, 4143, 2016.
12. M. J. Valero-Romero, G. J. Santaclara., L. Oar-Arteta, L. van Koppen, D. Y. Osadchii, J. Gascon, F. Kapteijn, *Chem. Eng. J.*, 360, 75, 2019.
13. O. Abuzalat, D. Wong, M. Elsayed, S. Park, S. Kim, *Sonochem*, 45,180, 2018
14. G. Lu, F. Chu, X. Huang, Y. Li, K. Liang, G. Wang, *Chem. Rev.*, 450, 214240, 2022.
15. M. Reza, M. Negar, M. Ashouri, *Iran. J. Sci. Technol. Trans. A Sci.*, 43, 443, 2019.
16. H. Asadevi, P. P. Nair, C. P. Amma, S. A. Khadar, S. C. Sasi, R. Raghunandan, *ACS Omega* 7, 13031, 2022.
17. Z. Z. Vasiljevic, M. P. Dojcinovic, J. D. Vujancevic, I. Jankovic-Castvan , N. B. Tadic, S. Stojadinovic, G. O. Brankovic, M. V. Nikolic, *R. Soc. Open Sci.* 7, 200708, 2025.
18. Q.V. Thi, M.S. Tamboli, Q. Thanh Hoai Ta, G.B. Kolekar, D. Sohn, *Mater. Sci. Eng. B.* 261, 114678, 2020.
19. K. Bhuvaneswari, G. Palanisamy, T. Pazhanivel, T. Maiyalagan, P. Shanmugam, A. N. Grace, *Chemosphere* 270, 128616, 2021.
20. A. Bhuyan, Md. Ahmaruzzaman, *Next Sustainability* 3, 100016, 2024.
21. B. Chen, X. Wang, Q. Zhang, X. Xi, J. Cai, H. Qi, M. Fang, 20(18), 3758, 2010.
22. H. Gupta, I. Saini, V. Singh, T. Kumar, V. Singh, *Bull. Chem. Reaction Engg. Catal.*, 19 (1),1, 2024.